Journal of Alloys and Compounds 645 (2015) S148–S151

Contents lists available at ScienceDirect

Journal of Alloys and Compounds

journal homepage: www.elsevier.com/locate/jalcom

Probing the cerium/cerium hydride interface using nanoindentation

Martin Brierley [a,b,*], John Knowles [a]

[a] Atomic Weapons Establishment, Aldermaston, Berkshire RG7 4PR, UK
[b] University of Manchester, Manchester M13 9PL, UK

ARTICLE INFO

Article history:
Available online 24 January 2015

Keywords:
Hydrogen absorbing materials
Metal hydrides
Rare earth alloys and compounds
Gas–solid reactions
Mechanical properties
Microstructure

ABSTRACT

A cerium hydride site was sectioned and the mechanical properties of the exposed phases (cerium metal, cerium hydride, oxidised cerium hydride) were measured using nanoindentation. An interfacial region under compressive stress was observed in the cerium metal surrounding a surface hydride that formed as a consequence of strain energy generated by the volume expansion associated with precipitation of the hydride phase.

1. Introduction

Various metals have the potential to form hydride phases. During extended periods of storage, environmental conditions can develop that enable the hydride phase to form. The formation of hydride phases has safety implications such as the potential to adversely change mechanical properties [1] and to cause unintended thermal excursions, pressurisations and/or breaches of containment [2–4]. To underwrite long-term storage, a predictive model of hydriding behaviour is desirable and requires detailed understanding. Investigating the growth kinetics and morphologies of metal hydride reaction sites is of fundamental importance to model development. Using cerium as an example of a hydride forming metal, this paper details the relative hardness and the extent of local stresses built up around a hydride reaction site.

An inconsistency exists between the morphology of cerium hydride sites found experimentally [5,6] and the lowest energy morphology predicted by Finite Element Modelling [7]. The calculations of Greenbaum et al. used elastic and elastic–plastic strain energy to predict the resulting shape for instantaneous formation of a surface hydride by obtaining the minimum strain energy of the system. The model suggests that hydride precipitates would be hemispherical when the hydride is harder than the metal, because the strain energy is incorporated within the softer matrix. With a thick oxide layer, a needle-like morphology with the long axis perpendicular to the surface was predicted. The calculation did not consider the influence that continued growth of the precipitated hydride site may impart to the final morphology.

Anisotropic growth kinetics that led to oblate hemispherical morphologies was demonstrated with cerium [5]. Vickers macro indentations demonstrated cerium hydride (2.2 GPa) to be significantly harder than cerium metal (0.34 GPa) [5]. Nanoindentation has been used on cerium metal to obtain similar hardness values (0.4 GPa) to the macro indentation [8]. A thin region of stressed material was found to surround the cerium sites. The Vickers indentations are too large to resolve the mechanical properties of this stressed region. Therefore, finer scale indentation methods are needed to probe the interface and investigate the mechanical properties of surface hydride features.

Cerium hydride reaction sites that have been exposed to air contain two layers, an oxidised hydride cap at the surface and a hydride in contact with the basal metal. Compressive stresses exist in the metal surrounding the hydride sites, sufficient to cause a phase change in the cerium surrounding a number of the reaction sites. It was suggested that the compressive stresses imparted into the surrounding cerium caused an isomorphic phase change from the γ-Ce to the α-Ce phase [6].

Nanoindentation on the cross section of a hydride site has been used to compare the hardness of the cerium metal, hydride and oxidised phases; and to investigate the strained material surrounding a hydride site. A sample of cerium was exposed to hydrogen to precipitate a small number of hydride sites (<20 sites) and was then cross sectioned. An environmental atomic force microscope (AFM) with a diamond cube corner indenter was used to probe the interface and investigate the mechanical properties of surface hydride features.

* Corresponding author at: Atomic Weapons Establishment, Aldermaston, Berkshire RG7 4PR, UK. Tel.: +44 118 9850938.
E-mail addresses: martin.brierley@awe.co.uk (M. Brierley), john.knowles@awe.co.uk (J. Knowles).

http://dx.doi.org/10.1016/j.jallcom.2015.01.116
0925-8388/

2. Method

2.1. Sample preparation and hydriding reaction

Sample preparation and subsequent hydriding at 10 mbar and 30 °C was performed as described previously [6]. The reacted sample was mounted edge-on in epoxy resin and sequentially ground and polished until a *ca.* 90 μm diameter hydride site was revealed. Experience with cerium metal mounted in epoxy resin has shown that no measurable oxidation of the sample occurs over that expected of the short air exposure during mounting. The sample was then polished using a 1 μm diamond suspension followed by 40 nm colloidal silica. The exposure of the sample to air following polishing was kept shorter than 60 s to minimise oxidation.

The cross section of the cerium hydride was imaged prior to the nanoindentation experiments using optical microscopy (Fig. 1) and a two layer hydride was confirmed.

2.2. Nanoindentation

Nanoindentation was performed using a Veeco Enviroscope™ atomic force microscope (AFM) evacuated to base pressure better than 8×10^{-4} Pa (6×10^{-6} Torr) with a Veeco PDNISP cube-corner diamond nanoindenter mounted on a stainless steel cantilever.

The dimensions of the nanoindenter cantilever were measured using a JEOL JSM 7000F Field Emission Gun Scanning Electron Microscope (FEGSEM) to have a length (L) of 315.4 μm, width (w) of 96.9 μm and thickness (t) of 12.9 μm. The actual spring constant (k) of the cantilever was calculated to be 323 N/m using $k = Ewt^3/4L^3$ [9]. The elastic modulus (E) of stainless steel was taken to be 195 GPa [10]. The diamond nanoindenter was imaged using the FEG-SEM following the indentations and the apex of the diamond tip was observed to be unchanged.

Cerium and cerium hydride are air sensitive and fresh surfaces are observed to tarnish during short air exposures (<10 min) [11]. Nanoindentation data would be affected by the presence of an oxide layer of because of the shallow sampling depth. Transfer of the sample following cross sectional polishing took less than 60 s from the final polish before the sample was evacuated.

A suitable load for the testing of the cerium metal was developed by performing indents at increasing cantilever deflections. A trigger threshold of 3 V, corresponding to a load of 0.4 mN, was found to be optimum for cerium metal.

A grid of 12 × 17 indentations was made near the centre of the hydride site at a uniform load of 0.4 mN. The grid was selected to ensure that indentations were made on the bulk metal, the stressed region, the hydride and the oxidised hydride. A further 12 × 17 grid was indented across an alternate area at a higher load of 1.35 mN (tip deflection 10 V).

3. Results and discussion

Height and phase maps were acquired using the nanoindenter cantilever in TappingMode™. The height map revealed a degree of differential polishing. The phase map of the hydride site indicates that each region had different material properties because different phase lag between driven and measured oscillations of the cantilever was measured for each region using TappingMode™; differing amounts of energy is lost per tip/surface interaction for each material type (Fig. 2).

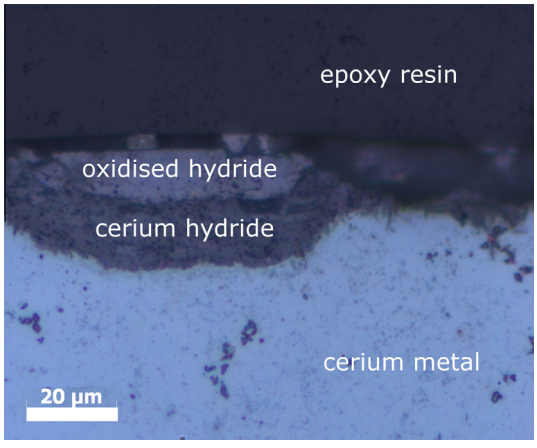

Fig. 1. An optical micrograph of the cerium hydride site prior to nanoindentation.

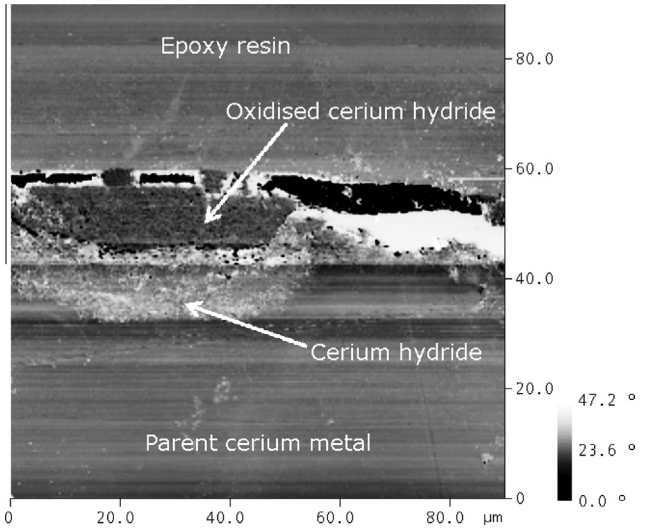

Fig. 2. The hydride phase is visible in the phase image of the cross section measured using tapping mode. The black areas correspond to a gap between the sample and the epoxy resin i.e. a free oscillation of the cantilever and the white areas are where the side of the tip has contacted the gap wall, leading to high losses by friction.

Grids of 12 × 17 nanoindentations at loads of 0.4 mN and 1.35 mN spanned the metal, interfacial region and hydride site, ensuring coverage of all the phases present. Fig. 3 shows the indents made for the 1.35 mN load. Average tip penetrations measured for the penetration depth at 0.4 mN load and the average relaxed indent depths for the relevant phases present are shown in Table 1. The difference between the penetration depths measured at load and the indent depths measured following removal of load and relaxation of the material was observed to be greater for the interfacial region than the bulk cerium metal. This indicates a greater degree of elastic recovery in the interfacial region suggesting that the region is under compressive stress as predicted by Greenbaum et al. [12]; the stress field extends 2–3 μm into the cerium from the hydride-metal interface. The same stress field was observed in the grid at 1.35 mN load; however at this load, the indents in the cerium metal overlapped, which prevented comparison between the metal and other phases.

The apparent hardness of the phases was calculated from the penetration depth measurements (h_c) from the 0.4 mN load (P) indentations using $H = P/A$ where the contact area $A = 2.597h_c^2$ [13]. The relative hardness of each phase compared to cerium metal is shown in Table 1. The hardness will be influenced by the presence of an oxide film. The short air exposure prior to indentation is likely to cause an oxide film of greater than 1 nm to form. The different phases may oxidise at different rates. This appears to have reduced the relative hardness of hydride to metal from 7 found using macro indentation to 1.7 using nanoindentation.

In this study and previously [1], the cerium hydride has been found to be significantly harder than the surrounding material yet an oblate morphology exists in contrast to the predictions of Greenbaum's model. Including sequences for continued growth into the calculations could improve the predictions for hydride morphology beyond the nucleation phase. Compressive stress will be generated by the large volume expansion (26.5%) associated with the precipitation of cerium hydride. Stressed cerium found surrounding a cerium hydride site of 90 μm in diameter at the surface is *ca.* 10–30 μm [1,2]. The interfacial region below a hydride site of similar size is 2–3 μm showing anisotropy in the thickness of the interfacial region (Fig. 4). This anisotropy can be explained by the expansion (relief) of the site out of the surface relieving

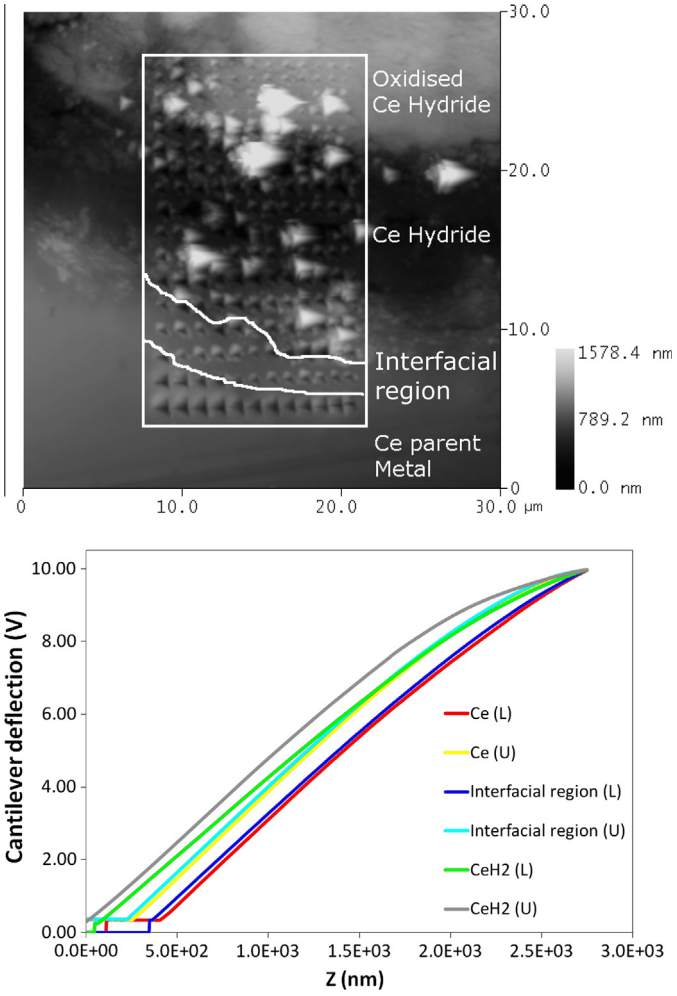

Fig. 3. Top: a height image of the grid of 12 × 17 nanoindentations made at a load of 1.35 mN covering the parent cerium metal across the cerium hydride and into the re-oxidised hydride. The load was selected to show up effectively in the hydride region, which caused impingement of the indents in the metal. Bottom: typical indentation traces for the cerium metal load (red) and unload (yellow), stressed (interfacial region) cerium load (dark blue) and unload (light blue), CeH_2 load (light green) and unload (dark green). There is a larger deflection for the stressed cerium compared to the unstressed cerium, but both load and unload traces are similar. A much larger deflection is observed for both the CeH_2 traces. All three traces converge at the trigger threshold of 10 V because the compliance of the cantilever becomes more significant as the contact area on the indent increases at high loads; this is calculated for when measuring indent penetration. (For interpretation of the references to colour in this figure legend, the reader is referred to the web version of this article.)

Table 1
The average penetration depths at load ($d_{0.4mN}$), the average relaxed indent depths (d_{relax}) and the apparent hardness relative (H_{rel}) to the cerium metal, (where $H_{rel} = H_{phase}/H_{Ce}$) are shown for each of the phases present in the cross sectioned reaction site.

	$d_{0.4mN}$ (nm)	d_{relax} (nm)	H_{rel}
Cerium metal	54 ± 12	42 ± 10	1
Interfacial region	59 ± 20	19 ± 11	0.9
Cerium hydride	47 ± 27	45 ± 32	1.69
Oxidised cerium hydride	35 ± 9	[a]	2.39

[a] The magnitude of d_{relax} for the oxidised hydride was similar to the magnitude of the surface topography and could not be measured.

most of the strain energy normal to the surface leaving a thin interfacial region of stress. Parallel to the surface the expansion is constrained by material on both sides, preventing relief of the strain

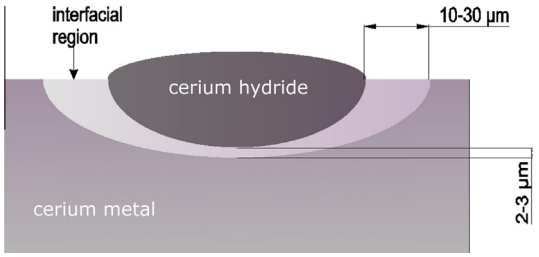

Fig. 4. A stylised cross section through a cerium hydride reaction site depicting the anisotropic interfacial region.

energy and resulting in a thicker interfacial region of stress close to the surface. The subsequent oxidation of the samples is unlikely to be responsible for the compressive stress imparted to the cerium metal because the unit cell volume of CeO_2 (0.160 nm^3) is smaller than that of CeH_2 (0.174 nm^3).

4. Conclusions

Cerium hydride has been shown to be significantly harder than cerium metal using nanoindentation. Significantly, the existence of an interfacial zone of cerium metal under compressive stress was observed surrounding the hydride site. The compressive stress field is generated by the large volume expansion (26.5%) associated with the precipitation of cerium hydride. The compressive stresses in the metal surrounding the hydride are anisotropic, with a larger extent near to the interface between the metal and the native oxide than under the hydride site. For a hydride of similar size to that measured in this study (*ca.* 90 µm) the size of the stress field surrounding the site laterally at the surface is typically 10–30 µm, but measured to be 2–3 µm beneath the hydride.

Acknowledgements

This work was funded by AWE plc via an EngD placement at the University of Manchester. Dr. D. Wheeler is acknowledged for discussions concerning nanoindentation.

References

[1] M. Ito, D. Setoyama, J. Matsunaga, H. Muta, K. Kurosaki, M. Uno, et al., Effect of electronegativity on the mechanical properties of metal hydrides with a fluorite structure, J. Alloys Comp. 426 (2006) 67–71, http://dx.doi.org/10.1016/j.jallcom.2006.02.036.
[2] D.H. Wood, S.A. Snowden, H.J. Howe, L.L. Thomas, D.W. Moon, H.R. Gregg, et al., Regarding the chemistry of metallic uranium stored in steel drums, J. Nucl. Mater. 209 (1994) 113–115.
[3] T. Totemeier, Characterization of uranium corrosion products involved in a uranium hydride pyrophoric event, J. Nucl. Mater. 278 (2000) 301–311, http://dx.doi.org/10.1016/S0022-3115(99)00245-7.
[4] J.M. Haschke, J.C. Martz, Catalyzed corrosion of plutonium: hazards and applications, Los Alamos Sci. 26 (2000) 266–273.
[5] J.P. Knowles, G. Rule, M. Brierley, The morphology and anisotropic growth kinetics of cerium hydride reaction sites, Corros. Sci. 77 (2013) 31–36, http://dx.doi.org/10.1016/j.corsci.2013.07.020.
[6] M. Brierley, J.P. Knowles, N. Montgomery, M. Preuss, The microstructure of cerium hydride growth sites, J. Vac. Sci. Technol. A 32 (2014) 031402.
[7] Y. Greenbaum, D. Barlam, M.H. Mintz, R.Z. Shneck, The strain energy and shape evolution of hydrides precipitated at free surfaces of metals, J. Alloys Comp. 452 (2008) 325–335, http://dx.doi.org/10.1016/j.jallcom.2006.11.045.
[8] D.W. Wheeler, J. Zekonyte, R.J.K. Wood, Mechanical properties of cerium and a cerium – 5 wt% lanthanum alloy by nanoindentation and ultrasonic velocity measurements, Mater. Sci. Eng. A 578 (2013) 294–302, http://dx.doi.org/10.1016/j.msea.2013.04.083.
[9] J.P. Cleveland, S. Manne, D. Bocek, P.K. Hansma, A nondestructive method for determining the spring constant of cantilevers for scanning force microscopy, Rev. Sci. Instrum. 64 (1993) 403, http://dx.doi.org/10.1063/1.1144209.

[10] L.I. Berger, Properties of solids, in: D.R. Lide (Ed.), CRC Handb. Chem. Phys, 88th ed., CRC Press, Boca Raton, Florida, 2008, p. 215.
[11] E.G. Zukas, R.A. Pereyra, J.O. Willis, The gamma to alpha phase transformation in cerium, Metall. Mater. Trans. A 18A (1987) 35–42.
[12] Y. Greenbaum, D. Barlam, M.H. Mintz, R.Z. Shneck, Elastic fields generated by a semi-spherical hydride particle on a free surface of a metal and their effect on its growth, J. Alloys Comp. 509 (2011) 4025–4034, http://dx.doi.org/10.1016/j.jallcom.2011.01.010.
[13] A.C. Fishcher-Cripps, Nanoindentation testing, in: Nanoindentation, Mechanical, Springer, 2011, pp. 21–38, http://dx.doi.org/10.1007/978-1-4419-9872-9.